Combined micro-Raman/UV-visible/fluorescence spectrometer for high-throughput analysis of microsamples

Jermim Noh
Department of Chemical and Biomolecular Engineering (BK21 Graduate Program), Korea Advanced Institute of Science and Technology, 373-1 Guseong-dong, Yuseong-gu, Daejeon 305-701, Korea and Center for Ultramicrochemical Process Systems, Korea Advanced Institute of Science and Technology, 373-1 Guseong-dong, Yuseong-gu, Daejeon, 305-701, Korea

Yung Doug Suh
Advanced Materials Division, Korea Research Institute of Chemical Technology, P.O. Box 107, Yuseong, Daejeon 305-600, Korea

Yong Ki Park
Division of Advanced Chemical Technology, Korea Research Institute of Chemical Technology, P.O. Box 107, Yuseong, Daejeon 305-600, Korea

Seung Min Jin
Advanced Materials Division, Korea Research Institute of Chemical Technology, P.O. Box 107, Yuseong, Daejeon 305-600, Korea

Soo Ho Kim and Seong Ihl Woo[a)]
Department of Chemical and Biomolecular Engineering (BK21 Graduate Program), Korea Advanced Institute of Science and Technology, 373-1 Guseong-dong, Yuseong-gu, Daejeon 305-701, Korea and Center for Ultramicrochemical Process Systems, Korea Advanced Institute of Science and Technology, 373-1 Guseong-dong, Yuseong-gu, Daejeon 305-701, Korea

(Received 16 October 2006; accepted 5 March 2007; published online 11 July 2007)

Combined micro-Raman/UV-visible (vis)/fluorescence spectroscopy system, which can evaluate an integrated array of more than 10 000 microsamples with a minimuma size of 5 μm within a few hours, has been developed for the first time. The array of microsamples is positioned on a computer-controlled *XY* translation microstage with a spatial resolution of 1 μm so that the spectra can be mapped with micron precision. Micro-Raman spectrometers have a high spectral resolution of about 2 cm^{-1} over the wave number range of 150–3900 cm^{-1}, while UV-vis and fluorescence spectrometers have high spectral resolutions of 0.4 and 0.1 nm over the wavelength range of 190–900 nm, respectively. In particular, the signal-to-noise ratio of the micro-Raman spectroscopy has been improved by using a holographic Raman grating and a liquid-nitrogen-cooled charge-coupled device detector. The performance of the combined spectroscopy system has been demonstrated by the high-throughput screening of a combinatorial ferroelectric (i.e., $BaTi_xZr_{1-x}O_3$) library. This system makes possible the structure analysis of various materials including ferroelectrics, catalysts, phosphors, polymers, alloys, and so on for the development of novel materials and the ultrasensitive detection of trace amounts of pharmaceuticals and diagnostic agents. © *2007 American Institute of Physics.* [DOI: 10.1063/1.2755745]

I. INTRODUCTION

In recent years, combinatorial and high-throughput methods have received much attention as innovative approaches to overcome the limitation of time-consuming conventional methods, leading to rapidly discovering novel materials,[1–5] catalysts,[1,6,7] pharmaceuticals,[8] and diagnostic agents.[9] As a representative example, Bruker AXS Inc. launched a high-throughput x-ray analysis tool (D8 DISCOVER CST) capable of analyzing many samples at high speed especially for a high growth area in the analysis of advanced materials, including drug discovery.

On the other hand, various other spectroscopic techniques are of vital importance for the purpose of qualitatively or quantitatively evaluating combinatorial libraries efficiently.[2,3,5,8–11] Recently, Gremlich[10] has reported that Raman (a complement to infrared spectroscopy) and diffuse reflection spectroscopies are useful analytical tools for high-throughput identification of combinatorial libraries and high-throughput monitoring of solid-phase reactions. Also, fluorescence spectroscopy as an extremely sensitive detection method has been applied to the optimization of a novel electroluminescent polymer and a photocatalyst,[2] high-throughput screening for drug discovery to employ fluorescence resonance energy transfer, fluorescence polarization, and fluorescence correlation spectroscopy,[8] and the rapid quantification of organic reactions directly on the resin.[10] These high-throughput techniques are individually adopted

[a)]Author to whom correspondence should be addressed; electronic-mail: siwoo@kaist.ac.kr

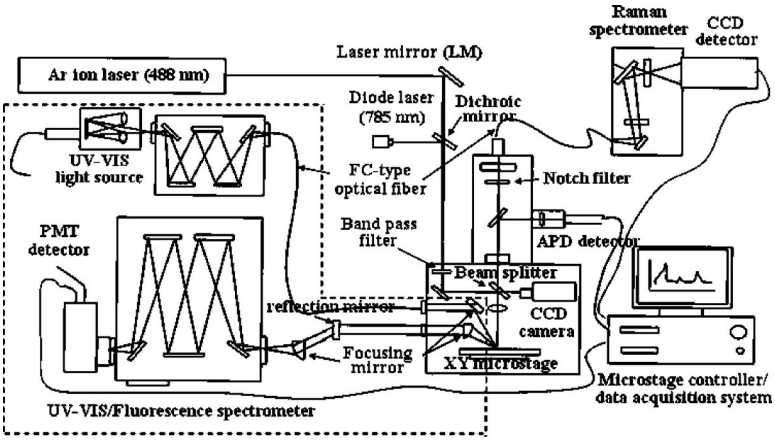

FIG. 1. Overall schematic drawing of the combined micro-Raman/UV-vis/fluorescence spectroscopy system. The dot line indicates the UV-vis/fluorescence spectroscopy system.

for the rapid analysis and characterization of combinatorial samples, and any integrated system has not been developed yet.

In this study, we present a combined system of micro-Raman, UV-visible (vis), and fluorescence spectroscopy, which makes possible high-throughput analysis of an integrated array of more than 10 000 microsamples in a few hours.

II. OVERALL DESCRIPTION OF COMBINED MICRO-RAMAN/UV-VIS/FLUORESCENCE SPECTROSCOPY SYSTEM

A schematic drawing of the combined micro-Raman/UV-vis/fluorescence spectroscopy system is described Fig. 1. The system consists of two parts, a micro-Raman spectroscopy system (Fig. 2) and a UV-vis/fluorescence spectroscopy system (Fig. 3). The latter allows UV-vis and fluorescence spectroscopies in turn. The samples of solid phases including thin films are positioned using a motorized *X-Y* stage controller with a step resolution of 1 μm and a manually focusing *Z* stage controller, and the allowable wafer sample size for mapping is a maximum of 4 in. [Figs. 2(c) and 3(c)]. The spectral data from two spectrometers are analyzed by using WINSPEC (WINSPEC/32, Roper Scientific) and DOUBLE-MONO (Dongwoo Optron Co.) softwares, respectively. In addition, a Si avalanche photodiode detector (APD) photon counting module (SPCM-AQR series, PerkinElmer Optoelectronics) with <250 dark counts/s and fiber-coupled receptacle is used for high sensitivity imaging of a luminescence library with micronscale patterns [Fig. 2(d)]. The detailed description of the two spectroscopic systems is as follows.

A. Micro-Raman spectroscopy system

The micro-Raman system adopts interchangeably two lasers, a 488 nm Ar ion laser (LS, Dynamic Laser) in the visible wavelength region and a 785 nm diode laser (BRM-785, B&WTEK Inc.) with a narrow linewidth of less than 0.02 nm in the near-infrared wavelength region [Fig. 2(a)]. The system includes an axial transmissive spectrograph (HoloSpec-$f/1.8i$, Kaiser Optical Systems, Inc.) with an appropriate holographic Raman grating (depending on the laser wavelength), coupled to a backilluminated, liquid-nitrogen-cooled charge-coupled device (CCD) detector (1340 $\times$400 pixels, Roper Scientific) [Fig. 2(a)]. The two laser beams are independently passed through a dichroic mirror, reflected by ultrabroadband silver-enhanced mirrors (OptoSigma) with a reflectance of more than 96.0% over the visible and near-infrared range, and then focused on the

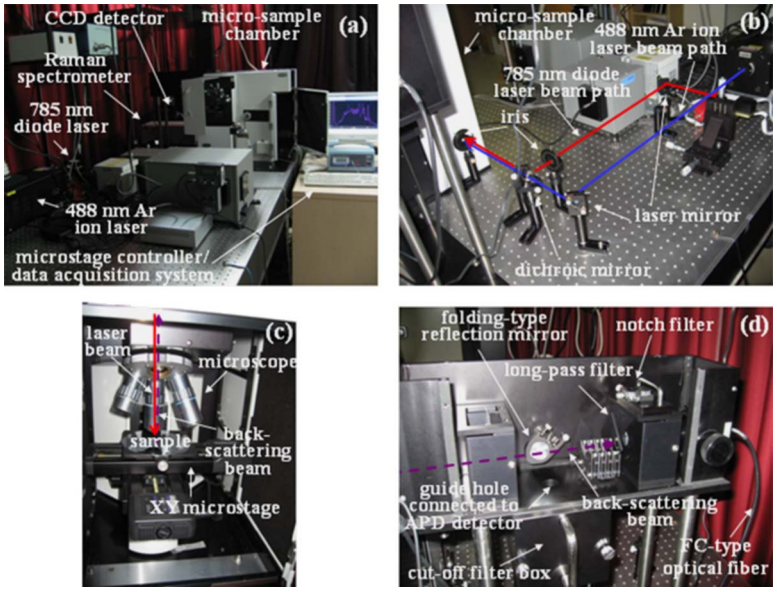

FIG. 2. (Color online) Detailed photographs of the micro-Raman spectroscopy system. (a) Side view of the system, (b) description of laser beam paths, (c) front view of the microsample chamber, and (d) side view of the filter box including a notch filter and a long-pass filter.

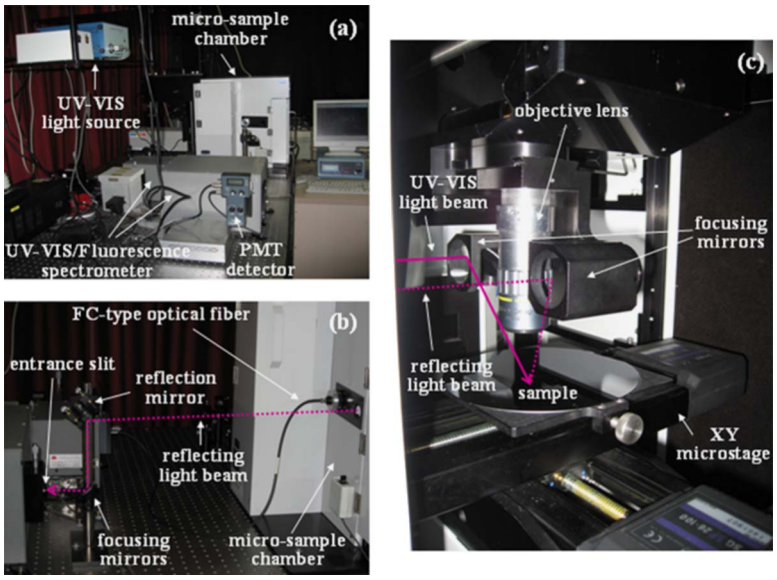

FIG. 3. (Color online) Detailed photographs of the UV-vis/fluorescence spectroscopy system. (a) Side view of the system, (b) description of UV-vis and reflecting light beam paths, and (c) side view of the microsample chamber including focusing mirrors.

sample by a micro-Raman microscope equipped with two Photon Design objectives [i.e., numerical aperture (NA) =0.7, M Plan 90×; NA=0.55, M Plan 45×] [Figs. 2(b) and 2(c)]. Raman-scattering radiation is collected by the micro-Raman microscope in the backscattering geometry, and then focused on the 25 (or 50 or 100) μm entrance slit of the spectrograph section via a multimode optical fiber (Laser Components, Inc.) with 200 μm core diameter, after being passed through a holographic notch filter (SuperNotch, Kaiser Optical Systems, Inc.) with narrow bandwidth of less than 350 cm^{-1} for Rayleigh scattering rejection [Fig. 2(d)]. In particular, for the near-infrared (NIR) Raman system with the excitation wavelength of 785 nm, the scattering light is collected through a 797 nm long-pass Raman filter (optical density >6 below 797 nm and transmission >90% above 800 nm, Omega Filters) with the steepest edge to completely reject the Rayleigh and anti-Stokes scattering. The data acquisition is performed using the analyzing software package WINSPEC in the wave number region from 200 to 4000 cm^{-1}. The laser beam size and power at the sample are minimum of 1 μm and maximum of 300 μW, respectively. Reference spectrum from compact Hg (for the 488 nm laser) or Ar (for the 785 nm laser) lamp (OptoSigma) is used for wavelength calibration.

B. UV-vis/fluorescence spectroscopy system

The UV-vis/fluorescence spectroscopy system is furnished with double monochromators for UV-vis and fluorescence spectroscopies [Fig. 3(a)]. A selectively switchable UV-vis light source consists of a deuterium lamp (C1518, Hamamatsu) in the wavelength region of 185–350 nm and a tungsten halogen lamp (Acton Research Corp.) in the wavelength region of 350–900 nm. The UV-vis/fluorescence spectrometer is equipped with a 150 mm focal length $f/4.7$ monochromator (DM-150, Dongwoo Optron Co.) with a 300 nm blaze grating (600 grooves/mm) for UV-vis spectroscopy and a 315 mm focal length $f/4.6$ monochromator (DM-320, Dongwoo Optron Co.) with a holographic grating blazed at 250 nm (1800 grooves/mm) for fluorescence spectroscopy. Incident UV-vis light passes a multimode optical fiber (Laser Components, Inc.) with 400 μm core diameter [Fig. 3(b)], and then it is focused on the target area of the sample by means of an optic assembly consisted of two parabolic aluminum mirrors coated with MgF_2 for receiving and focusing the light beam and a Photon Design objective (i.e., NA=0.28, M Plan 9×) [Fig. 3(c)]. As a result, the light beam is focused to a diameter of approximately 300 μm on the sample surface. The diffusely reflected photons are collected by using a reflective optics in an off-axis configuration with respect to the exit port of the microsample chamber, and then focused onto the entrance slit of the monochromator with the holographic grating (1800 grooves/mm) by using an additional focusing mirror (parabolic aluminum mirror) [Fig. 3(b)]. The adjustable slit width is 5 μm to 5 mm. Finally, the reflected photons are analyzed by using the Dong-Woo software (DOUBLE_MONO, Dongwoo Optron Co.) through a high-quantum-efficiency photomultiplier tube (PMT) detector (PDS-1, Hamamatsu) in which light energy is converted into electrical signal [Fig. 3(a)]. The parameter setting window in Fig. 4 shows the configuration and functionality of the DOUBLE-MONO software. In particular, the scan mode is set to "Reflectance" or "Absorbance" for UV-vis spectroscopy and "None" for fluorescence spectroscopy over the wavelength of 190–900 nm.

Especially for UV-vis spectroscopy, a $BaSO_4$ pellet (for powder samples) or an aluminum mirror coated with MgF_2 (for thin films) is used as a reflectance standard. In addition, the absorbance spectra of powder samples are based on the Kubelka-Munk (KM) function (F), which introduces the absorption coefficient (k) and scattering coefficient (s) to describe the reflectance (R) by[12]

$$F(R_\infty) = (1 - R_\infty)^2/2R_\infty = k/s, \quad (1)$$

where R_∞ is the infinite reflectance.

Mostly, not the absolute reflectance (R_∞) but reflectance relative to the standard (R_∞') is measured, and for a dilute species, the KM function is proportional to the concentration (c) of the species, similarly to the Lambert-Beer law[13] as

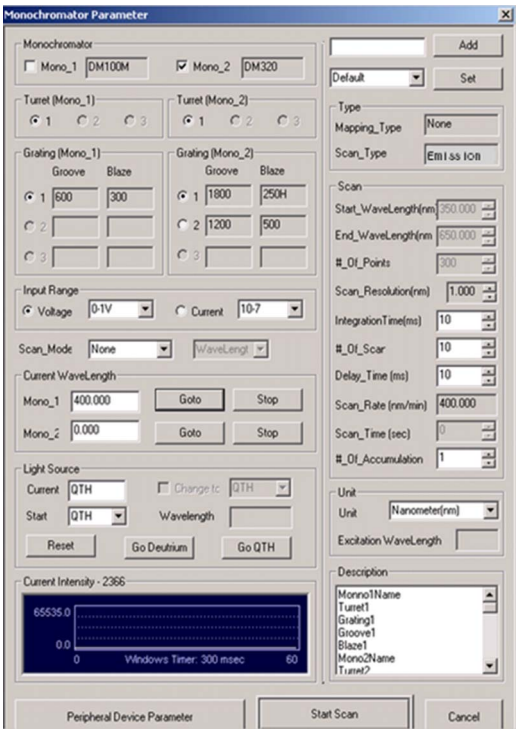

FIG. 4. (Color online) Parameter setting window of the DOUBLE-MONO software for the UV-vis/fluorescence spectroscopy.

$$F(R_\infty') \propto \varepsilon c/s, \tag{2}$$

where ε and s are the molar extinction and scattering coefficients, respectively.

III. CASE STUDY OF HIGH-THROUGHPUT ANALYSIS OF MICROSAMPLES

A. Preparation of a combinatorial library of ferroelectric thin films

An array of $BaTi_xZr_{1-x}O_3$ (BTZ) thin films was fabricated by using a multitarget radio frequency (rf)-sputtering system (SUNICOAT-524, Sunic System Co.) with two ceramic targets of $BaTiO_3$ and $BaZrO_3$ (purity: 99.999%). In order to vary the chemical composition of BTZ thin films, we deposited $BaTiO_3$ and $BaZrO_3$ on a (111) $Pt/TiO_2/SiO_2/Si$ substrate while moving the automated shutter back and forth, as shown in Fig. 5. The motion of the shutter was synchronized with plasma generation so that for each deposition cycle, a layer thickness gradient with respect to each target was created along the longitudinal axis of the Pt substrate surface. As shown in Fig. 6, the above deposition process was carried out ten times to obtain the combinatorial library of BTZ thin films with Ti concentration (x) within the range of 0–1 and a total layer thickness of about 100 nm. During the deposition process, the substrate temperature was kept at 300 °C to allow more efficient intermixing among the oxide layers. Additionally, a gas mixture of Ar and O_2 [$Ar/O_2=3:1$, total flow rate=20 SCCM (SCCM denotes cubic centimeter per minute at STP)] was used to suppress the formation of oxygen vacancies in the thin film library. Here, the process and bare pressures of the vacuum chamber were approximately 5×10^{-3} and 5×10^{-6} torr, respectively. After

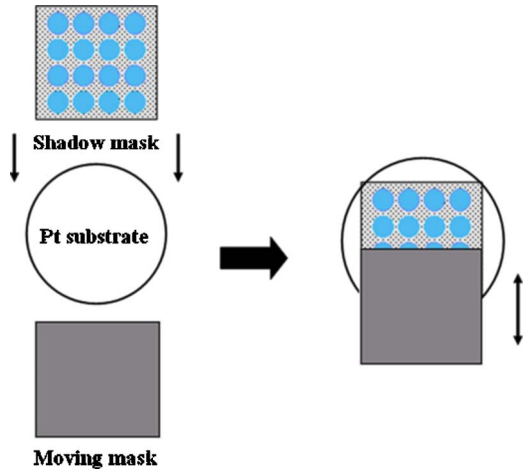

FIG. 5. (Color online) Fabrication scheme of the combinatorial library of $BaTi_xZr_{1-x}O_3$ thin films using the multitarget sputtering system equipped with an automated shutter.

the final deposition process, the BTZ thin-film library was postannealed in the tube furnace under oxygen flow at 650 °C for 1 h for crystallization.

In order to confirm efficient intermixing between two individual species (i.e., $BaZrO_3$ and $BaTiO_3$), we performed structural analysis of the BTZ thin-film library by using microbeam x-ray diffraction (XRD) (D8 DISCOVER GADDS (General Area Detector Diffraction System), Bruker-AXS). In contrast to the (110) diffraction peaks due to pure $BaZrO_3$ and $BaTiO_3$ thin films,[14] we clearly observed only one peak as well as peak-shift phenomena to higher diffraction angles in the 2θ range of 30°–32° as the Ti concentration (x) increases (data not shown). That is, the (110) diffraction peak of the thin-film library varies from 30.5° to 31.5° with the increase of the Ti content. Based on the results above, we can conclude that all samples of the BTZ thin-film library are single phase, indicating good intermixing between two individual species.[14]

B. Micro-Raman analysis of the combinatorial library of ferroelectric thin films

Figure 7 shows visible Raman spectra analyzed in the Ti concentration (x) range of 0–1. Here, we used the micro-Raman spectroscopy system equipped with a low-frequency holographic grating (entrance slit width=25 μm) covering a

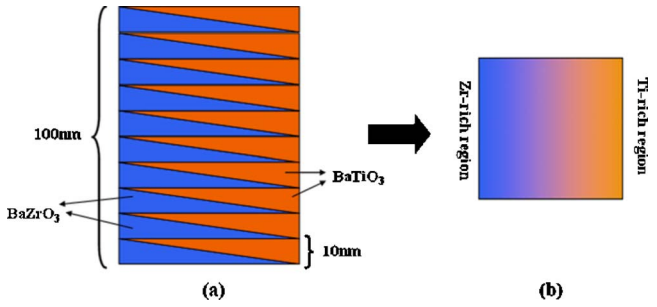

FIG. 6. (Color online) Schematic diagram of $BaTi_xZr_{1-x}O_3$ thin-film array prepared from $BaTiO_3/BaZrO_3$ multilayers using the multitarget sputtering system equipped with an automated shutter. (a) After ten deposition cycles (side view) and (b) after postannealing treatment (top view).

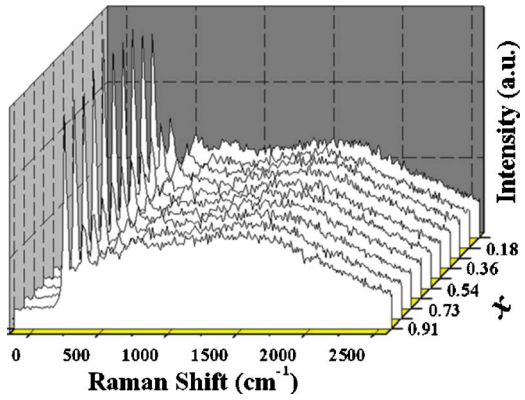

FIG. 7. (Color online) Micro-Raman spectra of $BaTi_xZr_{1-x}O_3$ thin-film array with the Ti concentration (x).

wave number range of about 2600 cm^{-1}. To obtain the micro-Raman spectra, the 488 nm Ar ion laser with a laser power of 40 mW was scanned in the longitudinal axis of the BTZ thin-film library by the computer-controlled program, and the integration time of all spectra was 10 s. Raman peaks due to ten BTZ thin films were clearly observed over the Raman shift range of 200–2600 cm^{-1}. Based on the corresponding CCD pixels (i.e., ~1170 pixels), the spectral resolution is calculated to be about 2 cm^{-1}/pixel. Furthermore, a combinatorial library of ferroelectric thin films with up to 1000 compositions could be analyzed within a few hours (i.e., 10 s/thin film).

IV. CASE STUDIES OF THE UV-VIS/FLUORESCENCE SPECTROSCOPY SYSTEM

A. Reflectance UV-vis spectroscopy of a fluorescent thin film

The reflectance UV-vis spectrum of a thin film of fluorescent dye Rhodamine 6G (R6G, Aldrich) was obtained using the monochromator with a 600 groove/mm grating of the UV-vis/fluorescence system. The R6G thin film (sample) was made by drop casting a 1 mM R6G solution (diluted with absolute ethanol) on a slide glass substrate. To remove the organic species of the surface, the substrate was cleaned with a piranha solution (3:1 mixture of sulfuric acid and 30% hydrogen peroxide). To obtain the reflectance UV-vis spectrum of the R6G thin film [Fig. 8(a)], slit widths of the entrance and exit slits and PMT voltage were set to be 20 μm and 400 V, respectively. For comparison, the reflectance spectrum of the glass substrate was also collected. As shown

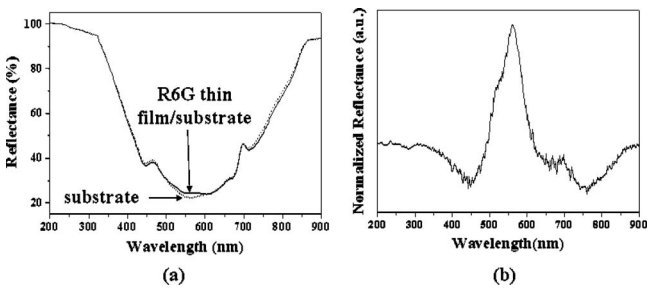

FIG. 8. Reflectance UV-vis spectrum (a) and normalized reflectance (b) of fluorescent R6G thin film on the slide glass substrate.

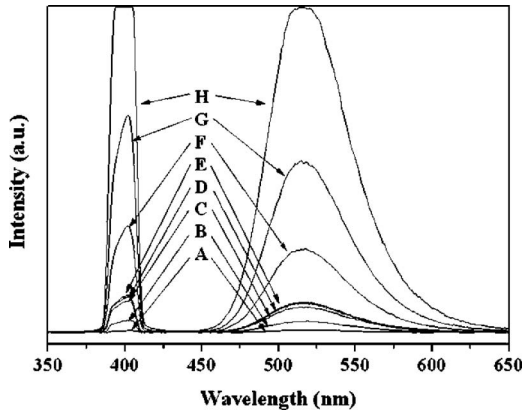

FIG. 9. PL emission spectra of Eu-doped barium strontium silicate ($BaSrSiO_4$) phosphor powder prepared by spray pyrolysis according to analysis conditions (A–H).

in Fig. 8(b), the calculated normalized reflectance is consistent with the absorption spectra of R6G film on quartz glass reported by Bryukhanov.[15] Here, the normalized reflectance was defined as a ratio of the reflectance from the R6G thin film/substrate and the reflectance from the glass substrate. Because the total analysis time per sample is about 1 min, a combinatorial library with up to 100 compositions could be analyzed within a few hours.

B. Photoluminescence (PL) spectroscopy of a phosphor powder

Figure 9 shows the PL emission spectra of Eu-doped barium strontium silicate ($BaSrSiO_4$) phosphor powder by changing the PMT voltage (500–600 V) and slit widths (0.1–5 mm) of the monochromator with a 1800 groove/mm grating of the UV-vis/fluorescence system. At first, the $BaSrSiO_4$ phosphor powder was prepared from a spray solution containing 5% NH_4Cl flux by spray pyrolysis according to the same recipe as reported by Kang *et al.*[16] With analysis conditions described in Table I, the PL emission spectra of the phosphor powder with an excitation wavelength of 400 nm were obtained. Here, the integration time corresponding to the decay time of the phosphor was set to be 10 ms. It is shown that as the PMT voltage and the slit widths increase, the luminescence emission intensity increases. Additionally, the emission wavelength of the phosphor powder at maximum peak intensity (i.e., λ_{max} =514 nm) is consistent with that reported by Kang *et al.*[16] Based on the resolution of the used double monochromator, the spectral resolution range of the UV-vis/fluorescence system is 0.1–0.4 nm.

TABLE I. Various analysis conditions for the photoluminescence spectroscopy of Eu-doped barium strontium silicate phosphor powder.

Analysis condition		A	B	C	D	E	F	G	H
Slit width (mm)	Entrance slit	0.1	1	1	1	2	5	5	5
	Exit slit	0.1	1	1	2	2	5	5	5
PMT voltage (V)		500		600		500		550	600

ACKNOWLEDGMENTS

This research was funded by the "Center for Ultramicrochemical Process Systems (CUPS)" sponsored by KOSEF (2004–2006). The authors thank Dr. Jaeyoun Kim and Professor Luke P. Lee from the "Biomolecular Nanotechnology Center" at the University of California-Berkeley for their technical assistance and useful discussions. Also, the authors thank Chang Hwa Jung and Hee Sang Kang from "CUPS" for their technical help.

[1] S. I. Woo, K. W. Kim, H. Y. Cho, K. S. Oh, M. K. Jeon, N. H. Tarte, T. S. Kim, and A. Mahmood, QSAR Comb. Sci. **24**, 138 (2005).
[2] P. Atienzar, A. Corma, H. García, and J. M. Serra, Chem.-Eur. J. **10**, 6043 (2004).
[3] R. A. Potyrailo and R. J. Wroczynski, Rev. Sci. Instrum. **76**, 062222 (2005).
[4] S. Anderson, Chem.-Eur. J. **7**, 4706 (2001).
[5] H. Jiu, J. Ding, J. Bao, Q. Zhang, and C. Gao, Spectrochim. Acta, Part A **61**, 3150 (2005).
[6] S. M. Senkan, Nature (London) **394**, 350 (1998).
[7] K. S. Oh, Y. K. Park, and S. I. Woo, Rev. Sci. Instrum. **76**, 062219 (2005).
[8] G. S. Sittampalam, S. D. Kahl, and W. P. Janzen, Curr. Opin. Chem. Biol. **1**, 384 (1997).
[9] J. Tu, Z. Yu, and Y.-H. Chu, Clin. Chem. **44**, 232 (1998).
[10] H.-U. Gremlich, Biotech. Bioeng. Comb. Chem. **61**, 179 (1998/1999).
[11] G. Gauglitz, Curr. Opin. Chem. Biol. **4**, 351 (2000).
[12] P. Kubelka and F. Munk, Physik **12**, 593 (1931).
[13] D. J. Swinehart, J. Chem. Educ. **39**, 333 (1972).
[14] F. M. Pontes, M. T. Escote, C. C. Escudeiro, E. R. Leite, E. Longo, A. J. Chiquito, P. S. Pizani, and J. A. Varela, J. Appl. Phys. **96**, 4386 (2004).
[15] V. V. Bryukhanov, J. Appl. Spectrosc. **70**, 450 (2003).
[16] H. S. Kang, Y. C. Kang, K. Y. Jung, and S. B. Park, Mater. Sci. Eng., B **121**, 81 (2005).